Article

Neural circuit mechanisms of sexual receptivity in *Drosophila* females

https://doi.org/10.1038/s41586-020-2972-7

Received: 13 January 2020

Accepted: 30 September 2020

Published online: 25 November 2020

Check for updates

Kaiyu Wang[1,3], Fei Wang[1,3], Nora Forknall[1], Tansy Yang[1], Christopher Patrick[1], Ruchi Parekh[1] & Barry J. Dickson[1,2]✉

Choosing a mate is one of the most consequential decisions a female will make during her lifetime. A female fly signals her willingness to mate by opening her vaginal plates, allowing a courting male to copulate[1,2]. Vaginal plate opening (VPO) occurs in response to the male courtship song and is dependent on the mating status of the female. How these exteroceptive (song) and interoceptive (mating status) inputs are integrated to regulate VPO remains unknown. Here we characterize the neural circuitry that implements mating decisions in the brain of female *Drosophila melanogaster*. We show that VPO is controlled by a pair of female-specific descending neurons (vpoDNs). The vpoDNs receive excitatory input from auditory neurons (vpoENs), which are tuned to specific features of the *D. melanogaster* song, and from pC1 neurons, which encode the mating status of the female[3,4]. The song responses of vpoDNs, but not vpoENs, are attenuated upon mating, accounting for the reduced receptivity of mated females. This modulation is mediated by pC1 neurons. The vpoDNs thus directly integrate the external and internal signals that control the mating decisions of *Drosophila* females.

Drosophila males woo potential mates by vibrating their wings to produce a species-specific courtship song. The male song induces deflections of the female aristae, thereby activating auditory sensory neurons that project to the central brain[5]. Several types of song-responsive neurons have been identified in the female brain[6–9], but it is unknown whether and how these neurons regulate sexual receptivity. How a female responds to the song of a male is highly dependent on whether or not she has previously mated. Once mated, females store sperm for days to weeks, and during this time are reluctant to mate again[10]. A male seminal fluid peptide (sex peptide) binds to sperm and signals the presence of sperm in the female reproductive tract through an ascending pathway from the sex peptide sensory neurons (SPSNs) in the uterus via the sex peptide abdominal ganglion (SAG) neurons in the ventral nerve cord to the pC1 neurons in the brain[3,4,11–13]. Sex peptide attenuates neuronal activity in the SPSN, SAG and pC1 neurons[4,13], thereby reducing sexual receptivity after mating[3,4,11–13]. We sought to investigate how these distinct external and internal signals are integrated in the female brain to control VPO (Supplementary Video 1), the motor output that signals the willingness of the female to mate.

Female receptivity is impaired by blocking the activity of the approximately 2,000 neurons that express either of the two sex-determination genes, *fruitless* (*fru*)[14,15] or *doublesex* (*dsx*)[16]. This class of neurons includes the *fru*$^+$ *dsx*$^+$ SPSNs[11,12], the *dsx*$^+$ SAGs[13] and the *dsx*$^+$ pC1 cells[3]. To search for other *fru*$^+$ or *dsx*$^+$ neurons that contribute to female receptivity, we screened a collection of 234 sparse driver lines specific for various *fru*$^+$ or *dsx*$^+$ cell types. We used these driver lines to genetically silence each of these cell types, and assayed virgin females for their frequency of copulation within 10 min of being individually paired with naive wild-type males (Extended Data Fig. 1). Of the seven lines with the strongest reduction in receptivity, two labelled the SPSNs, one labelled the SAGs and one labelled the pC1 cells. The other three lines targeted a pair of female-specific descending neurons, which we named vpoDNs (Fig. 1a, Extended Data Fig. 2a). These neurons are *dsx*$^+$, *fru*$^-$ and cholinergic (Extended Data Fig. 2b, c). Their dendrites arborize primarily in the lateral protocerebrum and their axons project to multiple regions of the ventral nerve cord, including the abdominal ganglion (Fig. 1a).

Acute optogenetic silencing or genetic ablation of the vpoDNs rendered virgin females unreceptive (Fig. 1b, Extended Data Fig. 3a), markedly reducing the frequency of VPO (Fig. 1c, Extended Data Fig. 3b) but not the intensity of male courtship (Extended Data Fig. 3c). Conversely, photoactivation of vpoDNs reliably triggered VPO in isolated virgin females (Fig. 1d, Extended Data Fig. 3d, Supplementary Videos 2, 3). We did not detect any peripheral expression driven by our vpoDN lines and by severing the abdominal nerve, confirmed that the VPO response is indeed due to activation of central neurons (Extended Data Fig. 3e).

Mated females are less receptive than virgins[10], which we found to correlate with a lack of VPO (Fig. 1e). To assess whether the failure to perform VPO accounts for the low receptivity of mated females, we photoactivated the vpoDNs in mated females as they were being courted by wild-type males. Whereas control females never copulated during a 1-h assay, approximately 30–50% of the vpoDN-activated females did remate (Fig. 1f). A similar remating frequency was observed upon vpoDN activation in mated females paired with wingless males, which court but cannot sing (Fig. 1f). Thus, direct activation of vpoDNs bypasses the need for both the internal state (virginity) and the external cue (song) that normally combine to elicit VPO.

[1]Janelia Research Campus, Howard Hughes Medical Institute, Ashburn, VA, USA. [2]Queensland Brain Institute, University of Queensland, St Lucia, Queensland, Australia. [3]These authors contributed equally: Kaiyu Wang, Fei Wang. ✉e-mail: dicksonb@janelia.hhmi.org

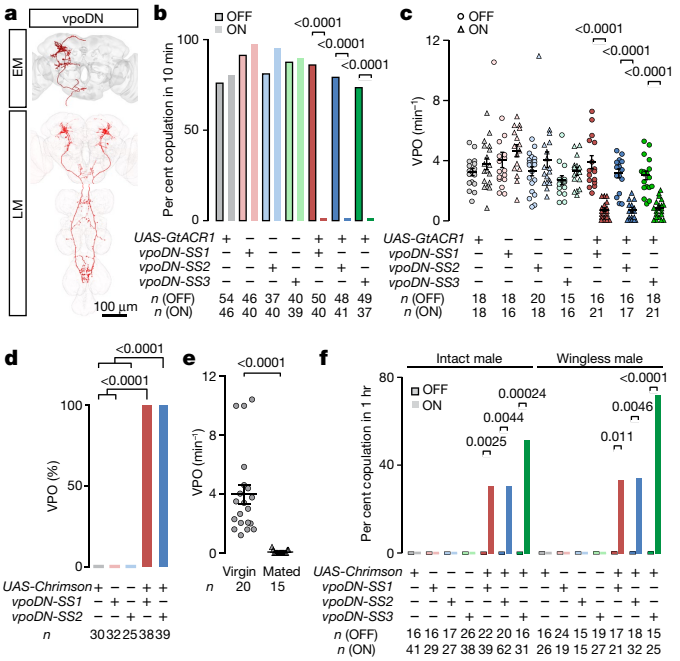

Fig. 1 | Female-specific vpoDNs control vaginal plate opening (VPO). **a**, Electron microscope (EM) reconstruction and confocal (LM) images of vpoDNs in the female central nervous system. **b**, **c**, Percentage of virgins copulating (**b**) and frequency of VPO (**c**) within 10 min of being paired with a wild-type male, with (ON) or without (OFF) constant optogenetic inhibition (560 nm, 10 µW mm^{-2} and 635 nm, 57 µW mm^{-2}). **d**, Percentage of isolated virgins exhibiting VPO upon photoactivation (5 s, 635 nm, 57 µW mm^{-2}). **e**, Frequency of VPO by wild-type females during a 10-min courtship assay. **f**, Percentage of mated females copulating within 1 h of courtship, with or without photoactivation (635 nm, 57 µW mm^{-2} in alternating 30-s ON–OFF periods). Data are mean ± s.e.m. *P* values indicated; two-sided Fisher's exact test in **b**, **d**, **f**; two-sided Wilcoxon test in **c**, **e**. See Supplementary Table 3 for details of statistical analyses.

We observed that wing extension is the most frequent male action just before female VPO (Extended Data Fig. 4a), and that both VPO and copulation rates are reduced if males are muted by removing their wings or females deafened by removing their aristae (Fig. 2a). These results suggested that the vpoDNs might be activated by male song. Indeed, in two-photon calcium-imaging experiments, we detected a robust increase of calcium levels in the neurites of vpoDNs in virgin females upon playback of male courtship song (Fig. 2b), but not in response to white noise (Extended Data Fig. 4b). The response to courtship song was lost when the aristae were immobilized to deafen the female (Fig. 2b). Song responses have also been reported for the pMN2 neurons[9], which are morphologically similar to vpoDNs and also *dsx*$^{+}$, although their reported functions differ[17] (Supplementary Information).

The vpoDN dendrites lie mostly in the superior lateral protocerebrum, with no obvious arborizations within the antennal mechanosensory centre (AMMC), the primary auditory neuropil, or in the wedge region, a secondary auditory neuropil known to include song-responsive neurons[7,8] (Fig. 1a). We therefore sought to trace potential pathways from these auditory centres to the vpoDNs within the electron microscopy volume of a full adult female brain[18] (FAFB). We identified a single vpoDN in each hemisphere and extensively traced the vpoDN in the right hemisphere (Fig. 1a, Supplementary Video 4) as well as its presynaptic partners, identifying a total of 45 neurons with at least 10 synapses impinging onto vpoDN (Extended Data Fig. 4c, Extended Data Table 1).

None of the vpoDN input neurons innervate the AMMC, but at least two cell types have extensive arborizations within the wedge (Fig. 2c, Supplementary Video 5). We obtained multiple split-GAL4 driver lines specific for these two cell types (Extended Data Fig. 5a). Fluorescence in situ hybridization predicted (Extended Data Fig. 5b), and whole-cell recording confirmed (Figs. 2d, e), that one of these cell types is excitatory and the other is inhibitory. Accordingly, we named these two cell types the vpoENs and vpoINs, respectively (Fig. 2c). Within FAFB there are two vpoEN cells and 14 vpoIN cells in each hemisphere.

We next performed optogenetic silencing and activation experiments to examine the roles of vpoENs and vpoINs in VPO and receptivity. Acute inhibition of the vpoENs significantly reduced the frequency of copulation (Fig. 2f) and VPO (Fig. 2g) when virgin females were paired with males. Conversely, strong optogenetic activation of vpoENs elicited VPO in isolated females (Fig. 2h), mimicking activation of vpoDNs (Fig. 1d). In virgin females paired with males, activating vpoINs suppressed mating (Fig. 2i) and VPO (Fig. 2j), whereas silencing vpoINs had no effect (Fig. 2f, g). Thus, vpoENs and vpoINs promote and suppress, respectively, both VPO and receptivity.

Using two-photon calcium imaging, we found that both vpoENs and vpoINs, as with vpoDNs (Fig. 2b), responded to playback of male courtship songs (Fig. 3). The courtship song varies considerably between different *Drosophila* species and is the primary cue the female uses for species recognition[19,20]. To test whether the vpoDNs, vpoENs and vpoINs are specifically tuned to the *D. melanogaster* courtship song, we presented natural courtship songs from seven other *Drosophila* species, selecting two representative audio clips from each species (Extended Data Fig. 6a). The vpoDNs showed little or no response to any of these songs, the vpoENs responded to one or two clips from five species, and the vpoINs responded to all but one clip from one species (Fig. 3, Extended Data Fig. 6b).

The *Drosophila* song comprises two main components: brief trains of high-amplitude pulses (pulse song) and continuous low-amplitude oscillations (sine song)[19]. The pulse song is the primary basis for species recognition[19,20], and in *D. melanogaster* consists of a series of pulses with an inter-pulse interval (IPI) of approximately 35 ms and a carrier frequency of 200–400 Hz (refs. [19–21]). We generated synthetic *D. melanogaster* pulse songs in which we systematically varied the IPI from 10 ms to 300 ms (Fig. 3a) and the carrier frequency from 100 Hz to 800 Hz (Extended Data Fig. 6c). Both vpoDNs and vpoENs responded robustly only to pulse songs with an IPI near 35 ms (Fig. 3b), and preferred lower carrier frequencies (Extended Data Fig. 6d). Neither vpoDNs nor vpoENs responded to white noise or synthetic sine song, even if its amplitude was increased to match that of the pulse song (Fig. 3b). The vpoINs were much more broadly tuned, responding to pulse songs across a wide range of IPIs (Fig. 3) and with higher carrier frequencies (Extended Data Fig. 6d). They also responded weakly to both sine song and white noise (Fig. 3b).

We also generated artificial pulse songs for each of the other species, again systematically altering the IPI from 10 ms to 300 ms (Fig. 3a, Extended Data Fig. 6e). Notably, the vpoDNs responded to the pulse songs of five other species once their IPI was shifted to match that of the *D. melanogaster* song (Fig. 3b, Extended Data Fig. 6f). Together, these data establish that the vpoDNs are finely tuned to the *D. melanogaster* pulse song, owing to their selectivity for an IPI of about 35 ms. This narrow tuning may arise through a combination of strong excitation from highly selective vpoENs and weak inhibition from broadly responsive vpoINs.

Having determined how auditory input controls VPO and sexual receptivity, we next examined how this response is modulated by the mating status of the female. VPO may be attenuated after mating either because the vpoENs and vpoDNs are less potent at eliciting VPO, or because they are less excited by song. In optogenetic activation and calcium-imaging experiments, we found that vpoDNs are equally potent in mated and virgin females (Fig. 4a), whereas both the basal calcium levels (Fig. 4b) and the response to courtship song (Fig. 4c) were lower in mated females than in virgins. By contrast, the vpoENs

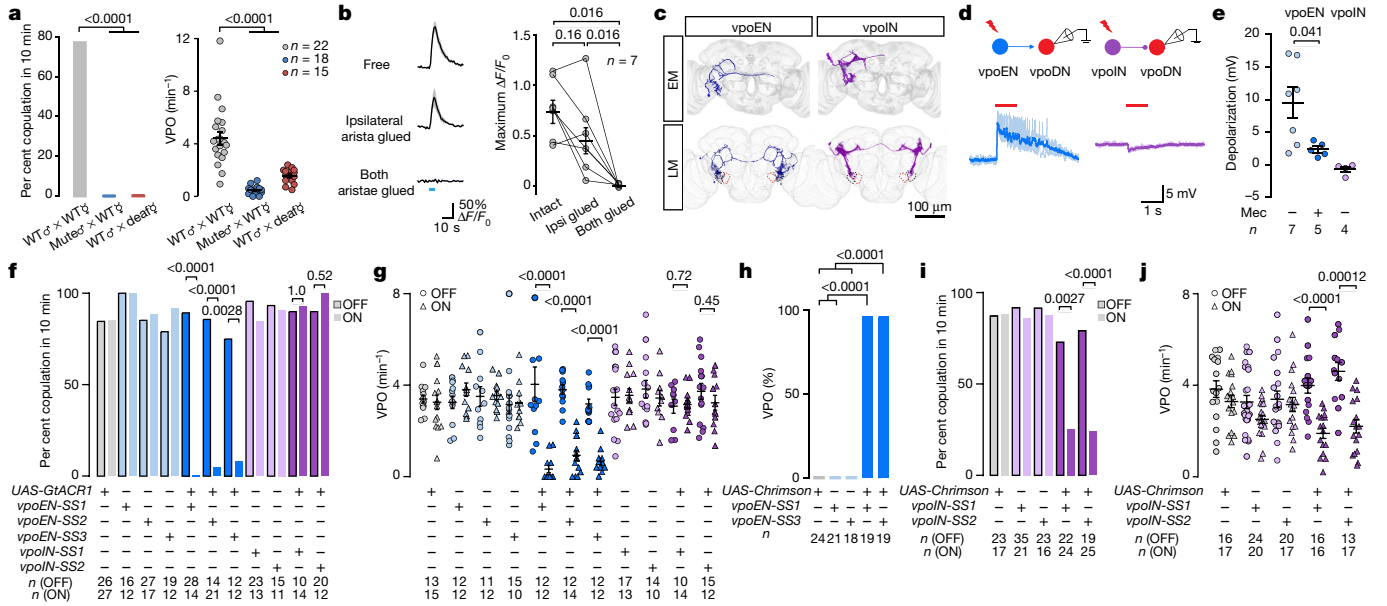

Fig. 2 | Auditory inputs to vpoDNs. a, Percentage of virgins copulating and frequency of VPO. **b**, Changes in signal from the calcium sensor GCaMP6s in vpoDNs in response to conspecific courtship song, with or without immobilization of aristae. Lines indicate data from the same fly. **c**, Electron microscopy reconstructions showing 2 vpoENs and 14 vpoINs in the right hemisphere, and confocal images showing 2 vpoENs and 7–8 vpoINs in each hemisphere. Dashed lines indicate AMMC (red) and wedge (black). **d**, Example traces of membrane potential changes in vpoDNs upon photoactivation (red bar) of vpoENs or vpoINs. **e**, vpoDN membrane potential changes upon photoactivation of vpoENs or vpoINs, before and after mecamylamine (mec) application. **f**, **g**, Copulation (**f**) and VPO (**g**) rates upon photoinhibition (560 nm, 10 μW mm^{-2} and 635 nm, 57 μW mm^{-2}), for virgins paired with wild-type males. **h**, Percentage of virgins exhibiting VPO upon vpoEN photoactivation (10 s, 635 nm, 57 μW mm^{-2}). **i**, **j**, Copulation (**i**) and VPO (**j**) rates upon vpoIN photoactivation (10 s, 635 nm, 57 μW mm^{-2}), for virgins paired with wild-type males. Data are mean ± s.e.m. *P* values indicated; two-sided Fisher's exact test in **a**, **f**, **h**, **i**; paired two-sided Wilcoxon test in **b**; unpaired two-sided Wilcoxon test in **e**, **g**, **j**. See Supplementary Table 3 for details of statistical analyses.

were significantly less potent at eliciting VPO in mated than in virgin females (Fig. 4a). Although basal fluorescence of vpoENs was slightly higher in mated females than in virgins, their song responses were indistinguishable (Fig. 4b, c). We also imaged calcium levels in vpoINs and found that the basal fluorescence and song responses of these cells were similar in mated and virgin females (Fig. 4b, c). Thus, these data show that vpoENs have a similar response to song in mated females as they do in virgins, but they are less able to excite vpoDNs in mated females.

The cell type with the most synaptic inputs to the vpoDNs was the pC1 cells (Fig. 4d, Extended Data Fig. 4c, Extended Data Tables 1, 2, Supplementary Video 5). Photoactivation of pC1 cells elicited a strong depolarization and action potentials in vpoDNs (Fig. 4e). The pC1 cells receive input from the SPSN–SAG pathway, which is silenced upon mating[4,13]. The reduced excitability of vpoDNs after mating may therefore be explained at least in part by the lower activity of pC1 cells[4], one of their major excitatory inputs. In support of this hypothesis, we found that acutely silencing either SAG or pC1 neurons reduced the frequency of VPO in virgin females to that of mated females (Fig. 4f). Conversely, photoactivation of pC1 cells in mated females restored both VPO (Fig. 4g) and sexual receptivity in response to courtship by intact but not wingless males (Fig. 4h). Moreover, transient (5-s) photoactivation of the pC1 neurons in mated females increased the sensitivity of vpoDNs to courtship song, demonstrating that pC1 cells control vpoDN excitability (Fig. 4i). This effect persisted for up to 25 s after photoactivation of pC1 cells (Fig. 4i).

We conclude that the decision of the female fly to mate or not to mate is largely determined by how the vpoDNs integrate signals from two direct synaptic inputs: the vpoENs, which are selectively tuned to the conspecific male courtship song, and the pC1 cells, which encode the mating status of the female (Fig. 4j). When the male sings, female vpoENs are activated; whether or not this leads to vpoDN activation and hence VPO depends on the level of pC1 activity, which is higher in

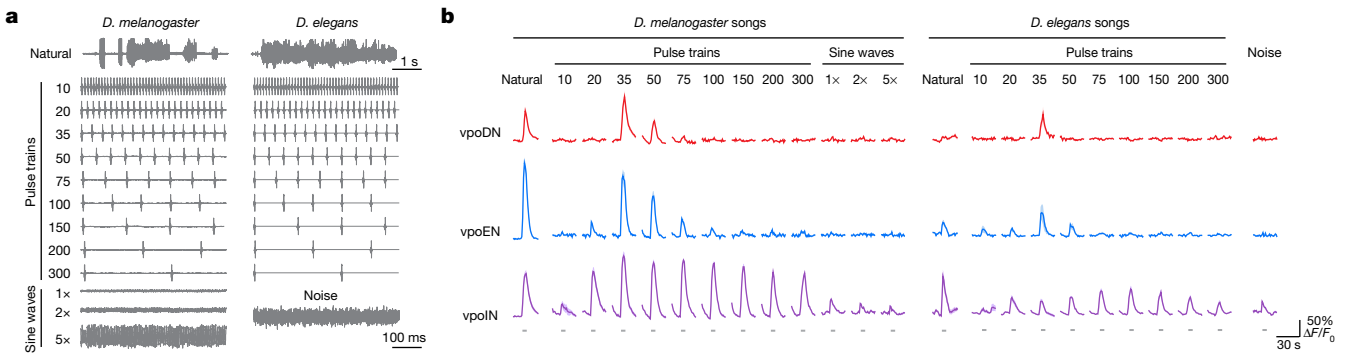

Fig. 3 | vpoENs and vpoDNs are tuned to conspecific courtship song. a, Traces of natural and synthetic *Drosophila* songs used as auditory stimuli. **b**, Sound-evoked GCaMP6s responses in vpoDNs, vpoENs and vpoINs of virgin *melanogaster* females ($n = 10–14$). Darker traces indicate mean response; lighter colours indicate s.e.m. Grey bars indicate stimuli (5 s).

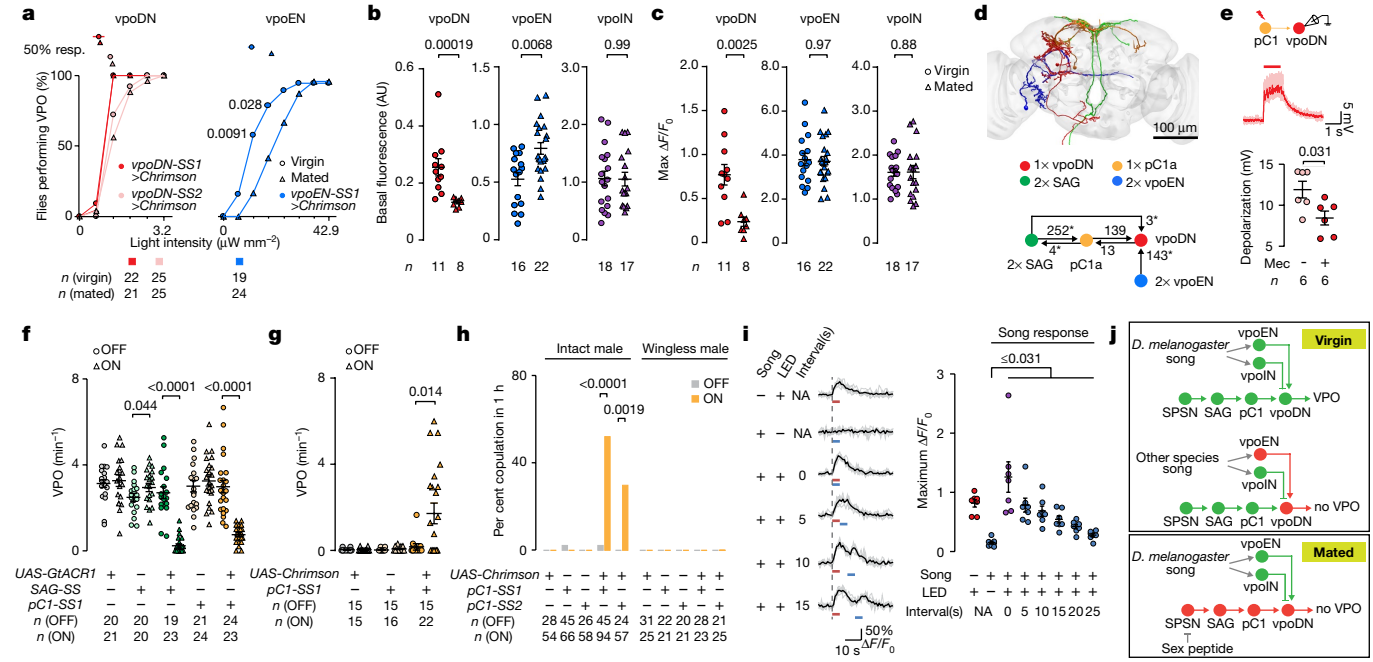

Fig. 4 | vpoDNs integrate mating status and song. a, Percentage of isolated flies exhibiting VPO upon photoactivation of vpoDNs (2 s, 635 nm) or vpoENs (10 s, 635 nm) at varying light intensities. Upper bars indicate 95% confidence intervals for the intensity eliciting a 50% response, derived from nonlinear regression. **b**, **c**, Basal (**b**) and song-evoked (**c**) GCaMP6s signals. **d**, Electron microscopy reconstructions of cell types and counts of impinging synapses. Asterisk indicates incomplete reconstruction. **e**, Membrane potential changes in vpoDNs upon photoactivation of pC1 neurons (red bar) before and after mecamylamine (mec) application. **f**, VPO frequency by virgin females during courtship with (ON) or without (OFF) constant optogenetic inhibition of SAG or pC1 neurons. **g**, **h**, VPO (**g**) and copulation (**h**) frequencies for mated females paired with wild-type males, with (ON, 635 nm, 57 μW mm^{-2}) or without (OFF) constant photoactivation of pC1 neurons. **i**, Example GCaMP6s traces (left) and plots (right) of responses in vpoDNs of mated females upon pC1 photoactivation (red) and song playback (blue) either alone or at varying delays ($n = 7$ flies). **j**, Model for the integration of song responses and mating status in vpoDNs. Data are mean ± s.e.m. *P* values indicated; two-sided Fisher's exact test in **a**, **h**; two-sided Wilcoxon test in **b**, **c**, **e**–**g**. See also Supplementary Table 3 for details of statistical analyses.

virgins than in mated females. The neural computation that underlies this state-dependent sensorimotor transformation remains to be determined; this will require methods for simultaneously manipulating and recording from all three cell types. One possibility is that the pC1 inputs gate the vpoEN inputs in a nonlinear fashion. We did not note any obvious spatial segregation of vpoEN and pC1 synapses onto the vpoDN dendrites, as might be expected if these inputs are indeed processed hierarchically. Alternatively, vpoDNs might simply use a sum-to-threshold mechanism, in which the combined input from vpoENs and pC1 s must exceed a certain level to elicit action potentials in vpoDNs. In this scenario, the lower pC1 activity after mating would necessitate a stronger vpoEN input to activate the vpoDNs. This model may account for the observation that wild-caught females are often multiply mated[22,23], consistent with the prediction from evolutionary theory that a mated female would increase her reproductive fitness by remating when she is courted by a male of higher quality than her first partner.

The many other, as yet uncharacterized, inputs to pC1, vpoEN and vpoDN cells may convey additional signals that modulate female receptivity. For example, pC1 cells are reported to respond to a male pheromone[3], which may serve to enhance the receptivity of both virgin and mated females. The persistent enhancement of vpoDN song responses upon transient activation of pC1 cells resembles the persistent state of courtship arousal induced in males by transient activation of the male pC1 counterparts[24,25]. The female pC1 cells may therefore encode both mating status and, as with their male counterparts, a lasting state of mating arousal induced by sensory cues from potential mates. The ensuing interaction between the two sexes involves a coordinated sequence of signals and responses, as exemplified by the male singing to elicit female VPO. In both sexes, these sensorimotor transformations may not be directly mediated by pC1 cells, as commonly thought[26], but rather modulated by the arousal states they encode. The neural architecture that we report here for the control of *Drosophila* female sexual receptivity may thus also serve as a paradigm for understanding male sexual behaviour, and perhaps more generally for the state-dependent signal processing that underlies behavioural decisions across a range of species.

Online content

Any methods, additional references, Nature Research reporting summaries, source data, extended data, supplementary information, acknowledgements, peer review information; details of author contributions and competing interests; and statements of data and code availability are available at https://doi.org/10.1038/s41586-020-2972-7.

1. Hall, J. C. The mating of a fly. *Science* **264**, 1702–1714 (1994).
2. Bussell, J. J., Yapici, N., Zhang, S. X., Dickson, B. J. & Vosshall, L. B. Abdominal-B neurons control *Drosophila* virgin female receptivity. *Curr. Biol.* **24**, 1584–1595 (2014).
3. Zhou, C., Pan, Y., Robinett, C. C., Meissner, G. W. & Baker, B. S. Central brain neurons expressing *doublesex* regulate female receptivity in *Drosophila*. *Neuron* **83**, 149–163 (2014).
4. Wang, F. et al. Neural circuitry linking mating and egg laying in *Drosophila* females. *Nature* **579**, 101–105 (2020).
5. Göpfert, M. C. & Robert, D. The mechanical basis of *Drosophila* audition. *J. Exp. Biol.* **205**, 1199–1208 (2002).
6. Kamikouchi, A. et al. The neural basis of *Drosophila* gravity-sensing and hearing. *Nature* **458**, 165–171 (2009).
7. Lai, J. S., Lo, S. J., Dickson, B. J. & Chiang, A. S. Auditory circuit in the *Drosophila* brain. *Proc. Natl Acad. Sci. USA* **109**, 2607–2612 (2012).
8. Vaughan, A. G., Zhou, C., Manoli, D. S. & Baker, B. S. Neural pathways for the detection and discrimination of conspecific song in *D. melanogaster*. *Curr. Biol.* **24**, 1039–1049 (2014).
9. Deutsch, D., Clemens, J., Thiberge, S. Y., Guan, G. & Murthy, M. Shared song detector neurons in *Drosophila* male and female brains drive sex-specific behaviors. *Curr. Biol.* **29**, 3200–3215 (2019).

10. Kubli, E. The sex-peptide. *BioEssays* **14**, 779–784 (1992).
11. Yang, C. H. et al. Control of the postmating behavioral switch in *Drosophila* females by internal sensory neurons. *Neuron* **61**, 519–526 (2009).
12. Häsemeyer, M., Yapici, N., Heberlein, U. & Dickson, B. J. Sensory neurons in the *Drosophila* genital tract regulate female reproductive behavior. *Neuron* **61**, 511–518 (2009).
13. Feng, K., Palfreyman, M. T., Häsemeyer, M., Talsma, A. & Dickson, B. J. Ascending SAG neurons control sexual receptivity of *Drosophila* females. *Neuron* **83**, 135–148 (2014).
14. Stockinger, P., Kvitsiani, D., Rotkopf, S., Tirián, L. & Dickson, B. J. Neural circuitry that governs *Drosophila* male courtship behavior. *Cell* **121**, 795–807 (2005).
15. Kvitsiani, D. & Dickson, B. J. Shared neural circuitry for female and male sexual behaviours in *Drosophila*. *Curr. Biol.* **16**, R355–R356 (2006).
16. Rideout, E. J., Dornan, A. J., Neville, M. C., Eadie, S. & Goodwin, S. F. Control of sexual differentiation and behavior by the *doublesex* gene in *Drosophila melanogaster*. *Nat. Neurosci.* **13**, 458–466 (2010).
17. Kimura, K., Sato, C., Koganezawa, M. & Yamamoto, D. *Drosophila* ovipositor extension in mating behavior and egg deposition involves distinct sets of brain interneurons. *PLoS ONE* **10**, e0126445 (2015).
18. Zheng, Z. et al. A complete electron microscopy volume of the brain of adult *Drosophila melanogaster*. *Cell* **174**, 730–743 (2018).
19. Ewing, A. W. & Bennet-Clark, H. C. Courtship songs of *Drosophila*. *Behaviour* **31**, 288–301 (1968).
20. Cowling, D. E. & Burnet, B. Courtship songs and genetic-control of their acoustic characteristics in sibling species of the *Drosophila-melanogaster* subgroup. *Anim. Behav.* **29**, 924–935 (1981).
21. Clemens, J. et al. Discovery of a new song mode in *Drosophila* reveals hidden structure in the sensory and neural drivers of behavior. *Curr. Biol.* **28**, 2400–2412 (2018).
22. Imhof, M., Harr, B., Brem, G. & Schlötterer, C. Multiple mating in wild *Drosophila melanogaster* revisited by microsatellite analysis. *Mol. Ecol.* **7**, 915–917 (1998).
23. Ochando, M. D., Reyes, A. & Ayala, F. J. Multiple paternity in two natural populations (orchard and vineyard) of *Drosophila*. *Proc. Natl Acad. Sci. USA* **93**, 11769–11773 (1996).
24. Bath, D. E. et al. FlyMAD: rapid thermogenetic control of neuronal activity in freely walking *Drosophila*. *Nat. Methods* **11**, 756–762 (2014).
25. Inagaki, H. K. et al. Optogenetic control of *Drosophila* using a red-shifted channelrhodopsin reveals experience-dependent influences on courtship. *Nat. Methods* **11**, 325–332 (2014).
26. Auer, T. O. & Benton, R. Sexual circuitry in *Drosophila*. *Curr. Opin. Neurobiol.* **38**, 18–26 (2016).

Methods

No statistical methods were used to predetermine sample size. The experiments were not randomized. The screening of 234 split-GAL4 lines (Extended Data Fig. 1) was performed and analysed by investigators blind to the genotype. All behavioural videos were analysed blind to the genotype. Calcium imaging and electrophysiology experiments were not performed blind to group allocation.

Flies

Flies were reared on standard cornmeal–agar–molasses medium, except for the females used for egg-laying test, which were kept on protein enriched food[27] after mating. Flies used in optogenetic experiments were supplied with 0.2 mM all-trans-retinal (Sigma-Aldrich) in food and reared in darkness, before and after eclosion. Flies were raised at 25 °C with relative humidity of about 50% and a 12 h:12 h light:dark cycle, unless otherwise noted. Flies stocks used in this study are described and listed in Supplementary Table 1, and full genotypes of flies used for experimental data presented in each figure are listed in Supplementary Table 2.

Split-GAL4 screening and stabilization

Split-GAL4 lines used in this study were generated and screened as previously described[4].

Neuron tracing in FAFB

We manually traced the neuron skeletons in a serial section transmission electron microscopy volume of the adult female *Drosophila* brain[18], using the annotation software CATMAID[28] (http://www.catmaid.org) as previously described[4]. We used confocal image stacks of the target cell types acquired with light microscopy as a guide to find and identify the same cell types in FAFB. We used neuroanatomical landmarks in the EM volume such as fibre tracts, cell body size and position, and neuropil boundaries to search for potential candidates of vpoDN. We looked for distinguishing features such as cell body position and tract orientation, and overall dendritic projection patterns in the confocal images. We then searched for corresponding areas of cell body position in the EM volume and followed the primary neurite emerging from the cell body as it formed fibre bundles and traversed the brain in an orientation that matched the data in the confocal images. We traced just enough of the primary and secondary neurites (backbone) of each potential candidate to compare with confocal data, and neurons that lacked prominent morphological features in the EM volume were eliminated from consideration. We identified synapses on these neurons using previously described criteria for a chemical synapse[18]. In brief, we marked instances in which vpoDN was postsynaptic indicated by the presence of postsynaptic densities (PSDs) on vpoDN and by the presence of a T-bar and vesicles at an active zone in the presynaptic partner across a synaptic cleft. After the vpoDN was traced to completion and all PSDs were marked, we used CATMAID's 'reconstruction sampler' tool to randomly select upstream partners of the vpoDN, which were then manually traced to identification. Using the sampler tool the reconstructed vpoDN skeleton was divided into intervals of 5,000 nm. Within each interval, the sampler lists the upstream or downstream connections of the neuron that were previously marked. The sampler selects a random synapse within a given interval, for which we identified the pre-synaptic T-bar and manually traced the neuron to which it belonged. All upstream partners were selected in this manner, and each was traced completely in the region of overlap with the vpoDN, and sufficiently to identify it.

Fluorescent staining and confocal imaging

Immunofluorescence staining[4] and fluorescent in situ hybridization[29] (FISH) were performed as previously described. In brief, polarity staining was used to determine the cell types labelled by a given split-GAL4 line, and multicolour stochastic labelling was performed to reveal morphology of individual cells. Detailed protocols for these two staining methods can be found online (https://www.janelia.org/project-team/flylight/protocols). For staining of Chrimson–tdTomato and GCaMP6, the central nervous systems were fixed in 4% paraformaldehyde (PFA; sc-821692, Santa Cruz, TX) at 22 °C for 15 min. After being washed in phosphate-buffered saline containing 0.5% (vol/vol) Triton X-100 (PBT) for 1 h at 22 °C, the samples were incubated in blocking buffer (50062Z, Thermo Fisher) containing primary antibodies with rabbit anti-dsRed (1:500, 632496, Takara Bio), chicken anti-GFP (1:500, A10262, Thermo Fisher), and mouse anti-Bruchpilot (nc82, 1:25, DSHB, IA) for 24–48 h at 4 °C. Then the samples were washed in PBT for 2–4 h before being incubated in blocking buffer containing secondary antibodies, which include AF488-conjugated goat-anti-chicken (1:300, A32931, Thermo Fisher), AF546-conjugated goat-anti-rabbit (1:300, A11035, Thermo Fisher), and AF647-conjugated goat-anti-mouse (1:300, A21235, Thermo Fisher) at 4 °C for 24 h. After being rinsed in PBT for 15 min at 22 °C, the samples were dehydrated and mounted on a slide. Confocal microscopy and image analysis were done as previously described[4].

Calcium imaging

The in vivo calcium imaging was performed on females aged 4–6 days using a customized two-photon microscope with ScanImage software (Vidrio Technologies) as previously described[4]. Sample preparation was as described, except that the two forelegs were immobilized by applying small amounts of UV curing adhesive (Loctite 352) to prevent them from touching the antennae. A loudspeaker was placed about 20 cm away from the back of the fly to play sound. To test whether song-evoked responses in vpoDNs require movement of the aristae, the same courtship song was presented to a single female with neither, one, or both aristae sequentially immobilized by applying a small amount of UV-curable adhesive to glue the arista to the cuticle. The songs were either recorded during fly courtship by using particle-velocity microphones (NR-23158, Knowles), or synthesized in MATLAB (Mathworks). Sound clips of 5 s length were played with 20 s or 40 s start-to-start intervals. Analysis of calcium-imaging data was done in Fiji[30] and MATLAB as previously described[4].

Electrophysiology

Whole-cell recordings were performed on central nervous system explants of 4-day-old females as previously described[4]. Data were collected using pCLAMP 10 software (Molecular Devices) with a Multiclamp 700B amplifier (Molecular Devices), low-pass filtered at 2 kHz and acquired at 10 kHz with a Digidata 1440A digitizer (Molecular Devices), and analysed offline in MATLAB (MathWorks).

Behavioural assays and analysis

The flies used in behavioural assays were collected, reared, and videotaped from above as previously described[4]. Videos were taken at 30 fps with a resolution of 0.02 mm per pixel unless otherwise noted. Infrared illumination (880 nm) as well as stimulations for optogenetic activation (635 nm, 57 $\mu W\ mm^{-2}$) or silencing (560 nm, 10 $\mu W\ mm^{-2}$, and 635 nm, 57 $\mu W\ mm^{-2}$) were provided from below. In experiments in which a female was paired with a male, low level of constant blue light (470 nm, 0.5 $\mu W\ mm^{-2}$) was provided for the flies to see each other.

The percent of copulation was calculated from the fraction of fly pairs that copulated within a 10-min or 1-h observation window. In the remating assay, virgin females aged 4 days were first paired individually with wild-type males for 1 h. Those females which finished copulating within this time were subsequently kept in fresh food vials in groups of 8–10 flies; those which did not copulate, or terminated copulation within 10 min, were discarded. Two days later, the mated females were paired individually with naive wild-type males, and the percentage of females copulating within 1 h was scored. In the remating assay in which pC1 neurons were photoactivated, a constant optogenetic activation

(635 nm, 57 μW mm^{-2}) was given. In remating assays in which vpoDNs were photoactivated, 30-s light pulses (635 nm, 57 μW mm^{-2}) were repeated 60 times with 30-s intervals.

For evaluating VPO by female flies, courtship chambers (diameter = 18 mm, height = 2 mm) were used to house single females or male–female pairs. VPO was identified as opening of the vaginal plates without any extension of the tube-like ovipositor (Supplementary Video 3). For examining VPO at higher resolution from the ventral side, females were chilled on ice for about 30 s, and glued on a glass with ventral side facing above. Small amounts of UV curing adhesive were applied at the back of thorax and back of abdomen to minimize the movement of the fly. In some flies, the hindlegs and cuticle over the posterior ventral nerve cord were removed with forceps to expose the abdominal ganglion and the abdominal nerve trunk. A small hook made from dissecting pin (26002-10, Fine Science Tools) was used to cut the exposed abdominal nerve trunk. The field-of-view of camera was zoomed in and focused at the tip of abdomen with a resolution of 1.8 μm per pixel. Female receptivity and egg-laying by females were carried out as previously described[4].

For annotating male behaviours around the onset of VPO by females, 10-min videos were manually analysed offline in Fiji. The onset of female VPO was defined as the frame in which the vaginal plates open. Wing extension was defined as frames in which the male extended its wings in a singing posture. Proboscis extension was defined as frames in which the male extended its proboscis to reach female's abdomen or genitalia. Abdomen bending was defined as frames in which the male bent its abdomen such that a line connecting the haltere and the abdominal tip came to meet at an angle of 15° or larger to the thoracic midline. Licking was defined as frames in which the male's proboscis touched female's genitalia. Holding was defined as frames in which the male held the female's abdomen with two forelegs. Copulation attempt was defined as the frame in which the male's genitalia touches the female's genitalia.

Statistical analysis

Female copulation and VPO frequencies were analysed using two-sided Fisher's exact tests. Egg-laying, calcium imaging, electrophysiology and all other behavioural data were analysed by unpaired two-sided Wilcoxon signed-rank tests unless otherwise noted. Stimulus intensities required to achieve a 50% response upon vpoDN or vpoEN activation were determined by fitting a sigmoidal curve using nonlinear regression. All analyses were performed using R software or MATLAB. To minimize clutter, only the most relevant statistical comparisons are presented in each figure. A full statistical analysis of all data are presented in Supplementary Table 3.

Reporting summary

Further information on research design is available in the Nature Research Reporting Summary linked to this paper.

Data availability

Confocal images of the central nervous systems of split-GAL4 lines used in this study are available at http://splitgal4.janelia.org/cgi-bin/splitgal4.cgi. Other datasets generated during the current study are available from the corresponding author on reasonable request.

27. Backhaus, B., Sulkowski, E. & Schlote, F. W. A semi-synthetic, general-purpose medium for *Drosophila melanogaster*. *Drosoph. Inf. Serv.* **60**, 210–212 (1984).
28. Schneider-Mizell, C. M. et al. Quantitative neuroanatomy for connectomics in *Drosophila*. *eLife* **5**, e12059 (2016).
29. Meissner, G. W. et al. Mapping neurotransmitter identity in the whole-mount *Drosophila* brain using multiplex high-throughput fluorescence in situ hybridization. *Genetics* **211**, 473–482 (2019).
30. Schindelin, J. et al. Fiji: an open-source platform for biological-image analysis. *Nat. Methods* **9**, 676–682 (2012).

Acknowledgements We thank the Janelia FlyLight, Fly Facility, Project Technical Resources, Molecular Biology, Functional Connectome, and Experimental Technology teams and N. Chen for technical assistance; E. Lillvis, E. Behrman and D. Stern for providing courtship songs of various *Drosophila* species; and K. Svoboda, K. Feng and K. Keleman for comments on the manuscript. This work was funded by the Howard Hughes Medical Institute.

Author contributions B.J.D., K.W. and F.W. conceived the study and wrote the manuscript. K.W. and F.W. performed all experiments and analysed the data. N.F., T.Y., C.P. and F.W. reconstructed selected neurons and synapses in the FAFB EM volume. R.P. managed the tracing team.

Competing interests The authors declare no competing interests.

Additional information

Supplementary information is available for this paper at https://doi.org/10.1038/s41586-020-2972-7.

Correspondence and requests for materials should be addressed to B.J.D.

Peer review information *Nature* thanks the anonymous reviewer(s) for their contribution to the peer review of this work.

a

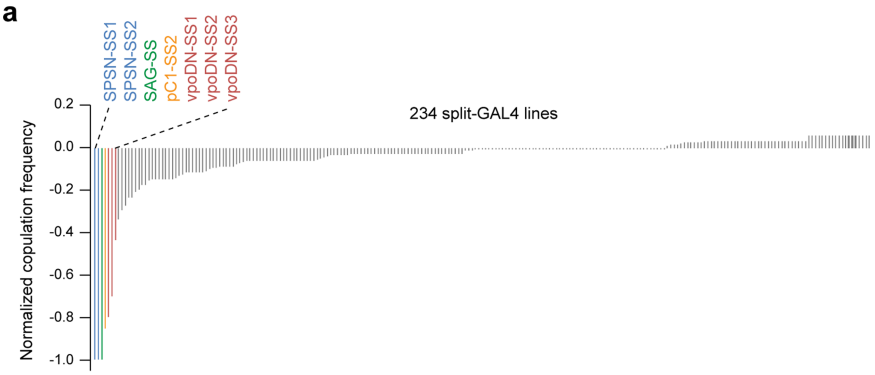

b

No.	SS ID	n	No.	SS ID	n	No.	SS ID	n	No.	SS ID	n
	control	36	59	31680	36	118	1458	34	177	59829	31
1	50910	36	60	45431	36	119	50948	35	178	45449	36
2	50911	36	61	45498	36	120	45434	35	179	56922	32
3	51118	36	62	58835	27	121	3365	35	180	59823	34
4	59911	36	63	59855	36	122	31662	35	181	61091	34
5	50200	31	64	60207	36	123	56867	36	182	41514	35
6	53451	28	65	59853	36	124	2997	35	183	50269	35
7	50795	28	66	59915	36	125	1520	36	184	3602	35
8	53457	24	67	45441	28	126	32548	35	185	35134	35
9	50931	36	68	43627	29	127	59874	35	186	50917	35
10	60199	35	69	59830	31	128	60198	35	187	4505	35
11	45451	36	70	59859	33	129	59916	35	188	45427	35
12	60200	36	71	3049	35	130	60193	35	189	45486	35
13	59900	36	72	45406	35	131	45525	35	190	60196	35
14	50893	25	73	45471	35	132	57876	35	191	60192	35
15	3302	36	74	1440	35	133	50945	18	192	45437	36
16	53456	36	75	25718	35	134	50943	36	193	45427	36
17	59838	25	76	61093	35	135	34692	36	194	45424	36
18	31695	36	77	50915	36	136	31692	18	195	35672	36
19	48166	36	78	50946	36	137	50920	36	196	3511	36
20	45490	36	79	45435	36	138	33847	36	197	3607	36
21	31674	36	80	45499	36	139	3627	36	198	50940	36
22	59854	36	81	50921	36	140	31691	36	199	3326	36
23	53454	31	82	45512	36	141	31679	36	200	1506	36
24	50942	31	83	50933	36	142	32542	36	201	45470	36
25	60213	32	84	50936	36	143	45489	18	202	3209	36
26	3298	33	85	3104	36	144	56824	36	203	31661	36
27	60202	23	86	45510	36	145	56857	36	204	32549	36
28	50937	36	87	3283	36	146	56902	36	205	45502	29
29	50938	36	88	3369	36	147	3112	36	206	60194	36
30	31701	36	89	3493	36	148	3558	36	207	60205	36
31	1489	36	90	1463	36	149	45512	36	208	44448	36
32	41548	36	91	31700	36	150	3054	36	209	60212	36
33	3108	36	92	31697	36	151	31676	36	210	59882	36
34	45449	25	93	56822	36	152	1441	36	211	59905	36
35	60189	33	94	3563	36	153	1502	35	212	59909	36
36	38356	35	95	2996	36	154	3006	36	213	45407	35
37	59902	35	96	31655	36	155	3103	36	214	45443	36
38	50939	36	97	33795	36	156	31964	36	215	50913	26
39	40401	36	98	1504	36	157	33828	36	216	50258	36
40	31664	36	99	33850	36	158	50913	36	217	40414	36
41	60201	36	100	45443	33	159	41741	18	218	4668	35
42	59887	36	101	45497	36	160	3215	36	219	21695	18
43	45498	31	102	59826	36	161	45441	36	220	45461	36
44	60190	33	103	60195	36	162	59871	36	221	45430	18
45	45446	34	104	60208	36	163	45448	36	222	31659	35
46	50895	26	105	61092	36	164	59831	36	223	3573	36
47	59841	26	106	59840	36	165	59837	36	224	2982	36
48	50947	35	107	59846	36	166	60206	36	225	33842	32
49	45479	35	108	59883	36	167	61090	36	226	3044	36
50	45415	35	109	59913	36	168	60191	36	227	3080	18
51	45227	36	110	59891	36	169	59848	36	228	3398	17
52	43274	36	111	60197	30	170	57878	36	229	45507	36
53	48743	36	112	61089	30	171	1916	22	230	59869	21
54	31678	36	113	57877	30	172	60210	23	231	59820	31
55	45518	36	114	59908	32	173	3915	24	232	60204	36
56	3453	36	115	33872	33	174	59888	24	233	59898	36
57	31685	36	116	59872	33	175	50922	28	234	1892	23
58	3003	18	117	50926	34	176	1519	31			

Extended Data Fig. 1 | Genetic screen for neuronal activities required for female receptivity. a, Difference in the copulation frequencies of split-GAL4 *UAS-TNTe* (tetanus toxin) and control *UAS-TNTe* virgin females within a 10-min observation period, relative to the control group. **b**, Stable-split lines (SS ID) and sample size (*n*) for the 234 split-GAL4 lines shown in **a**.

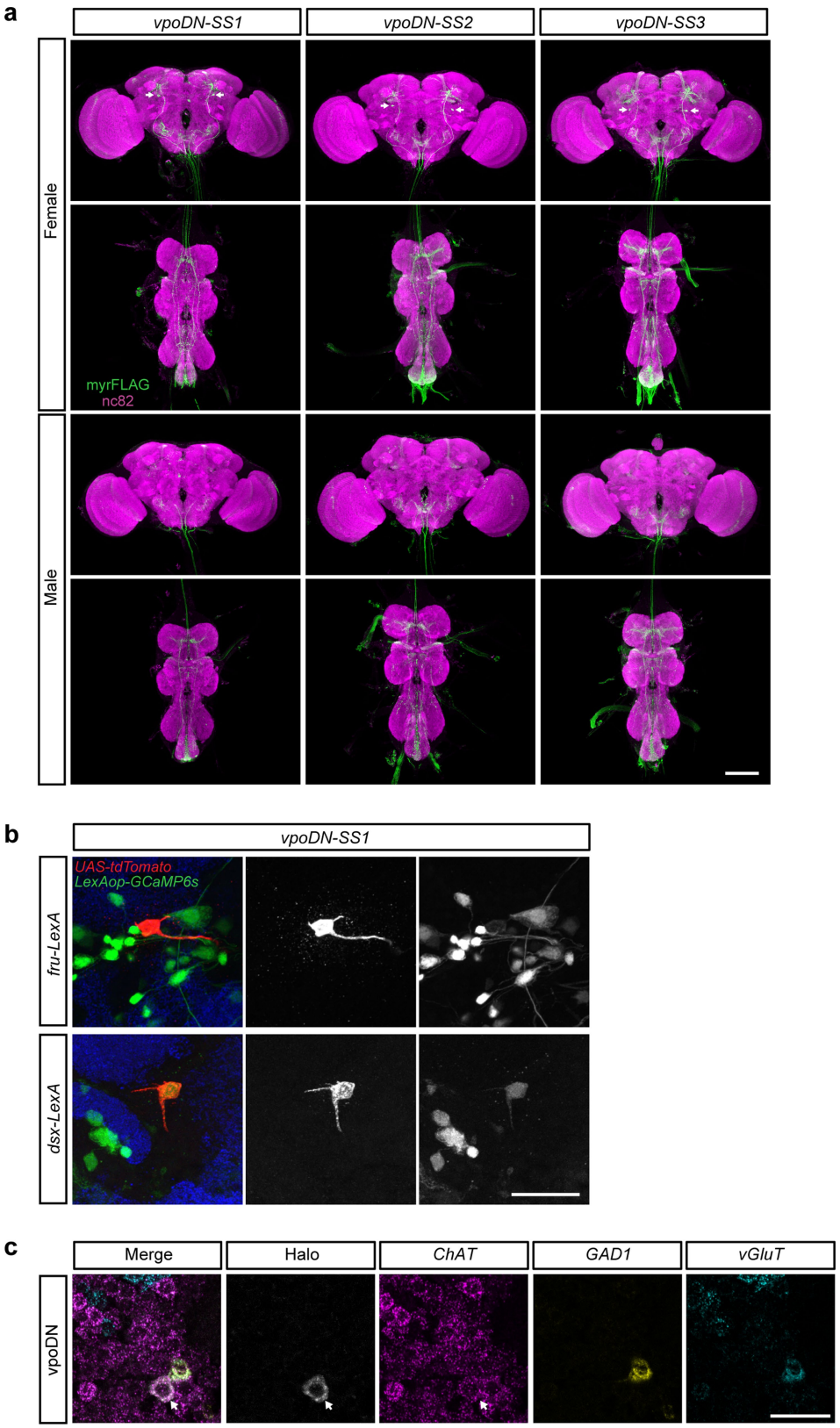

Extended Data Fig. 2 | Anatomical characterization of vpoDNs. a, Confocal images of brains and ventral nerve cords from female and male flies carrying *vpoDN-SS1*, *vpoDN-SS2*, or *vpoDN-SS3*, and *UAS-myrFLAG*, stained with anti-FLAG to reveal membranes of targeted neurons (green) and mAb nc82 to reveal all synapses (magenta). One pair of vpoDNs are labelled in females but not in males. Scale bar: 100 µm. **b**, Confocal images of female brains showing the co-labelling of vpoDNs with *dsx-LexA* but not *fru-LexA*. Scale bar: 20 µm. **c**, Confocal images of female brains showing the expression of *ChAT*, *GAD1*, and *vGluT* in vpoDN (labelled by Halo tag, arrows), as revealed by FISH. Scale bar: 10 µm. Representative images are shown from at least 5 independent samples examined in each case.

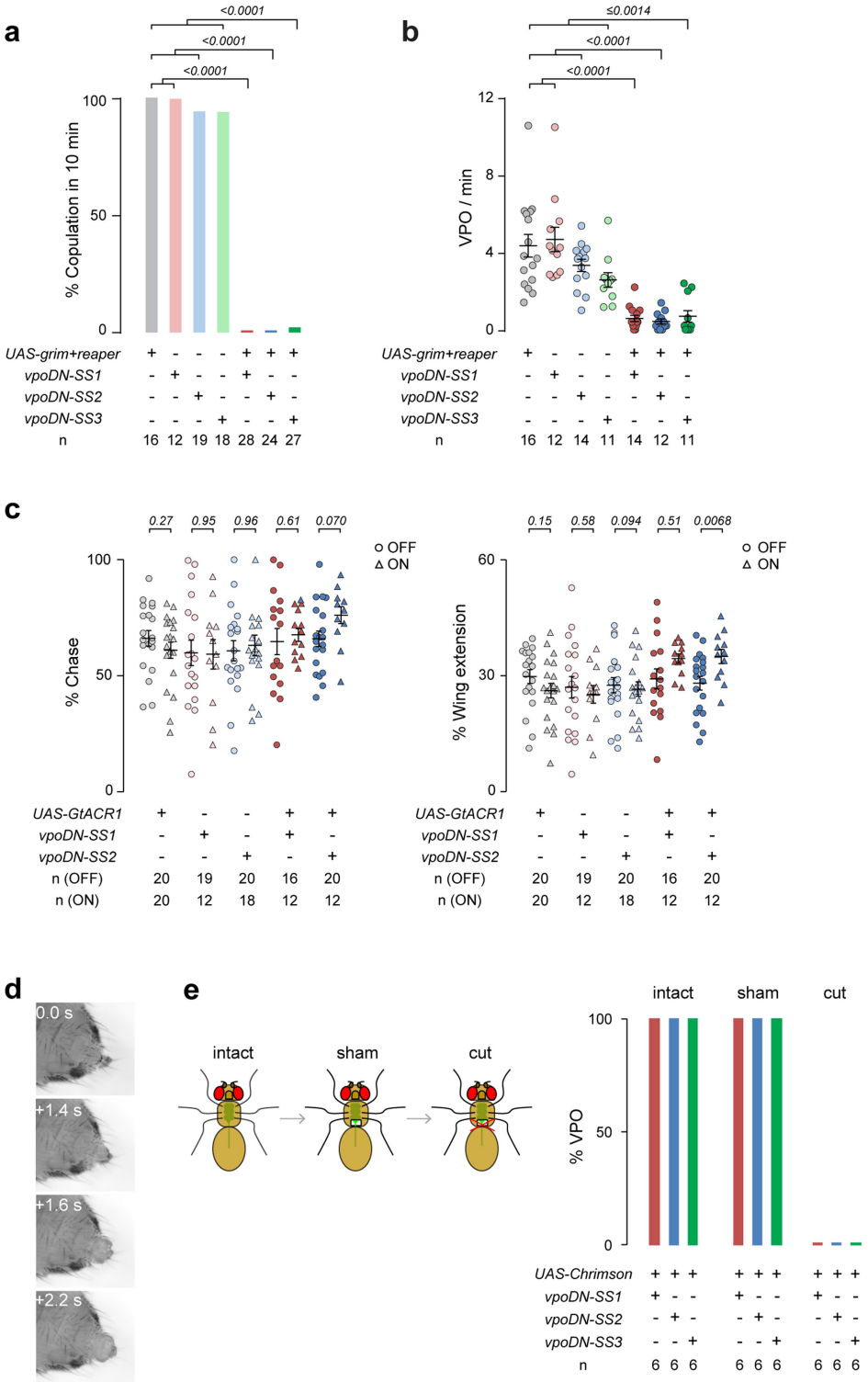

Extended Data Fig. 3 | Functional characterization of vpoDNs. **a**, **b**, Percentage of pairs copulating (**a**) and frequency of VPO (**b**) during 10 min of courtship between a virgin female of the indicated genotype and a wild-type male. **c**, Percentage of time wild-type males chased or extended their wings towards the virgin female during a 10-min observation period. **d**, Snapshots of female VPO induced upon photoactivation of vpoDNs (Supplementary Videos 2, 3). **e**, Percentage of isolated virgins performing VPO upon photoactivation of vpoDNs (5 s, 635 nm, 57 μW mm^{-2}). Each female was tested three times as follows: first, while intact, then with the cuticle over the posterior part of ventral nerve cord removed to expose the abdominal ganglion (sham), and finally, after the abdominal nerve trunk was severed (cut). Data in **b** and **c** shown as scatter plots with mean ± s.e.m. *P* values in italics, two-sided Fisher's exact test in **a**, two-sided Wilcoxon test in **b** and **c**. See Supplementary Table 3 for details of statistical analyses.

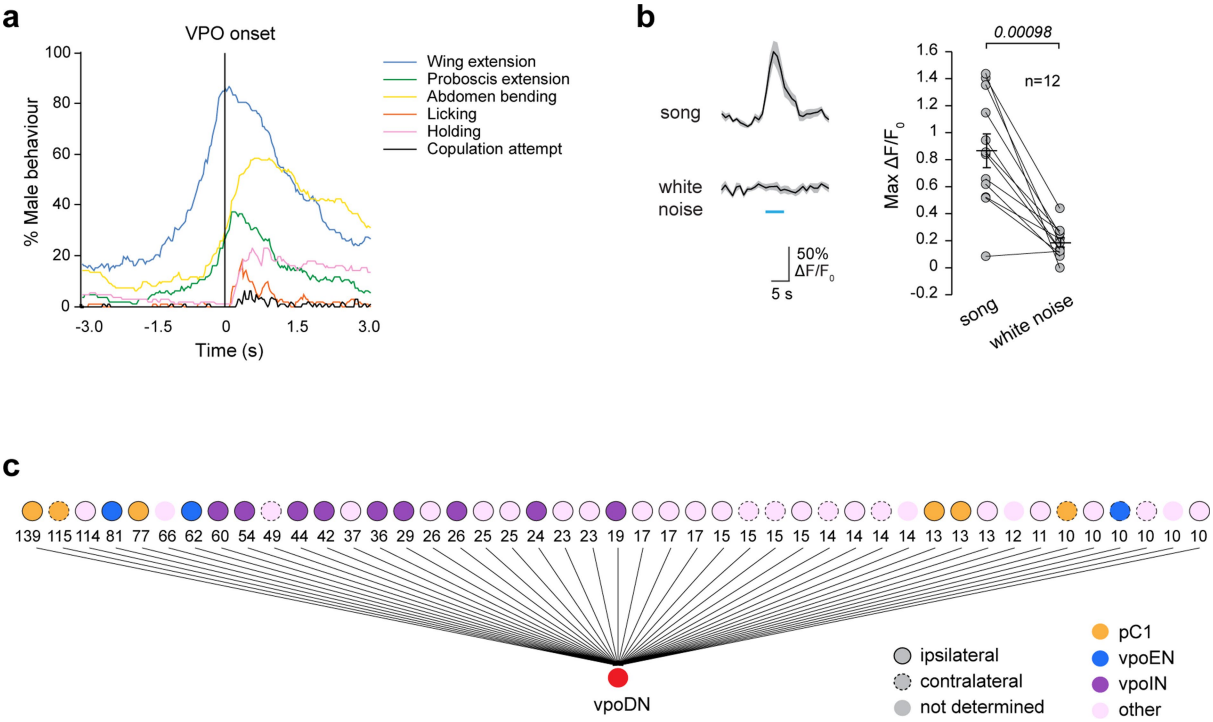

Extended Data Fig. 4 | vpoDNs are sensitive to courtship song and are postsynaptic to auditory neurons. a, Frequency of male courtship behaviours around the onset of female VPO. *n* = 124 VPOs from 12 pairs of flies. **b**, GCaMP6s signal changes in vpoDNs of virgins with intact aristae in response to courtship song and white noise. Lines connect data points from the same fly. Error bars show mean ± s.e.m. *P* values in italics, paired two-sided Wilcoxon test. See also Supplementary Table 3. **c**, Neurons presynaptic to a single vpoDN in the FAFB EM volume, showing the number of input synapses identified (thresholded at 10).

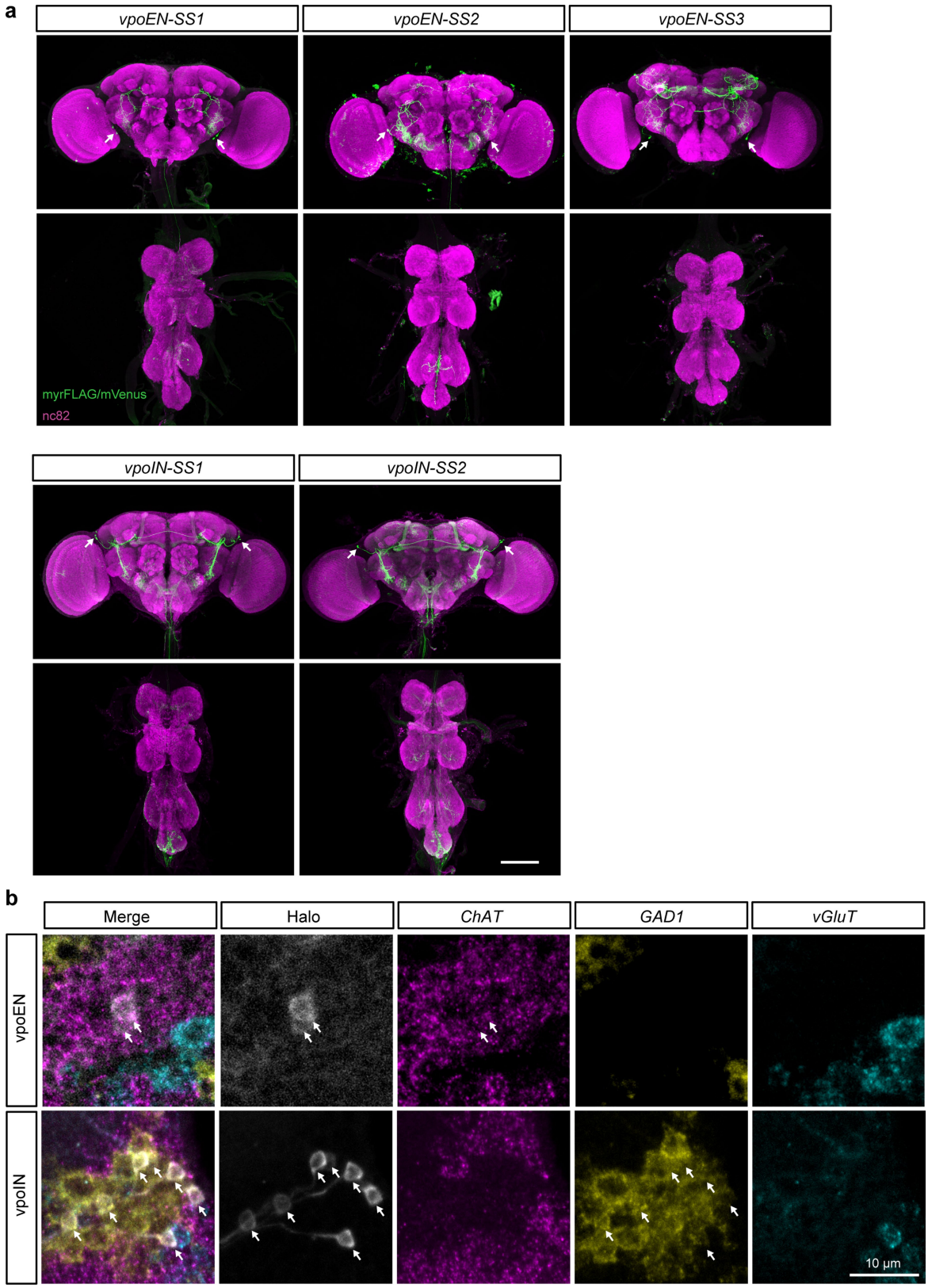

Extended Data Fig. 5 | Split-GAL4 driver lines targeting vpoENs and vpoINs and neurotransmitter types revealed by FISH. a, Confocal images of female central nervous system carrying indicated split-GAL4 driver lines and *UAS-myrFLAG* or *UAS-Chrimson-mVenus*. Samples were stained with anti-FLAG or anti-GFP (green) to reveal membranes of targeted neurons and mAb nc82 to reveal all synapses (magenta). Arrows indicate soma. Scale bar: 100 µm. **b**, Confocal images showing the expression of *ChAT*, *GAD1*, and *vGluT* in vpoEN and vpoIN neurons (labelled by Halo tag, arrows) in female brains, as revealed by FISH. Representative images are shown from at least 5 independent samples examined in each case.

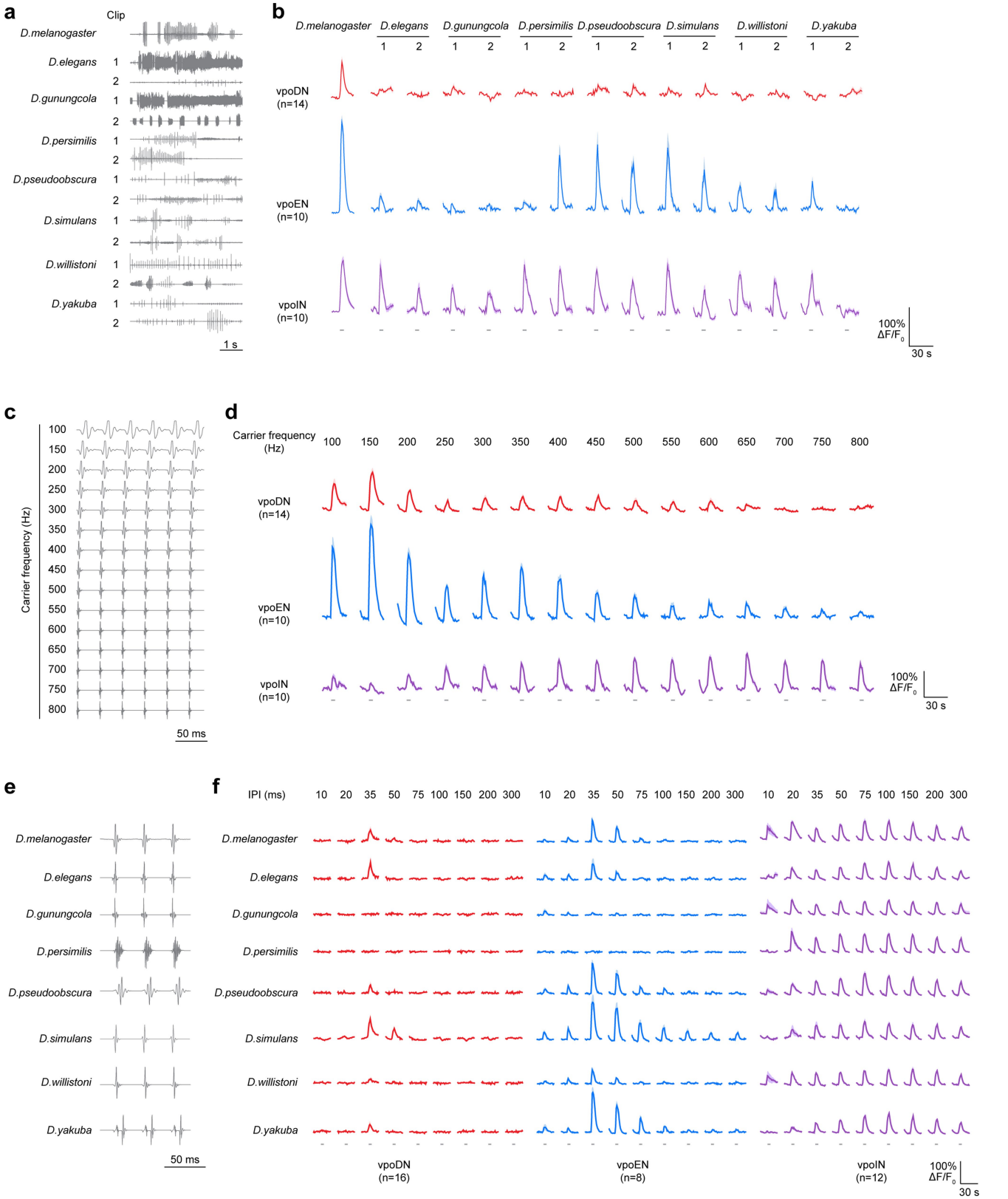

Extended Data Fig. 6 | Responses of vpoDN, vpoEN, and vpoIN towards natural and synthetic courtship songs. a, **c**, **e**, Traces of natural and artificial songs used as auditory stimuli. **b**, **d**, **f**, Sound-evoked GCaMP6s responses in vpoDNs, vpoENs and vpoINs of virgin *melanogaster* females. Darker traces indicate mean response; grey shading indicates s.e.m. Grey bars indicate stimuli (5 s). '1' and '2' in **a** and **b** indicate different audio clips from the same species. Selected data for *Drosophila elegans* are reproduced in Fig. 3. Sample sizes were as indicated, except for responses to *simulans* songs, for which $n = 7$, 6 and 6 for vpoDN, vpoEN, and vpoIN, respectively.

Extended Data Table 1 | vpoDN inputs identified by EM reconstruction

Cell ID	Hemisphere	Cell type	vpoDN (5094165)
3807213	R	pC1a	139
3838016	L	pC1a	115
5787563	R		114
5496947	R	vpoEN	81
3794184	R	pC1c	77
7965359	N.D.		66
5480915	R	vpoEN	62
5114793	R	vpoIN	60
6481209	R	vpoIN	54
5934095	L		49
5310407	R	vpoIN	44
5486635	R	vpoIN	42
6170157	R		37
1945493	R	vpoIN	36
5500623	R	vpoIN	29
6068590	R		26
7125206	R	vpoIN	26
2135548	R		25
5557175	R		25
5753207	R	vpoIN	24
3397581	R		23
5297515	R		23
5592797	R	vpoIN	19
5105812	R		17
6185015	R		17
6051130	R		17
6764899	R		15
7124679	L		15
6913699	L		15
6172298	R		15
3205032	L		14
6105481	R		14
5174016	L		14
7404025	N.D.		14
3781622	R	pC1b	13
3778246	R	pC1d	13
8551397	R		13
8275720	N.D.		12
8125540	R		11
3837770	L	pC1d	10
5153878	R		10
5874280	L	vpoEN	10
5888229	L		10
7957672	N.D.		10
7979198	R		10

Number of synaptic connections identified between various input neurons and the right hemisphere vpoDN (threshold 10 synapses). R and L indicate soma location in right (ipsilateral) or left (contralateral) hemisphere; N.D., soma not identified.

Extended Data Table 2 | Synaptic connections identified by EM reconstruction

		Post																							
Pre	**Cell ID**	**SAG_R**	**SAG_L**	**pC1a**	**pC1b**	**pC1c**	**pC1d**	**pC1e**	**vpoDN**	**vpoEN_R1**	**vpoEN_R2**	**vpoIN_R1**	**vpoIN_R2**	**vpoIN_R3**	**vpoIN_R4**	**vpoIN_R5**	**vpoIN_R6**	**vpoIN_R7**	**vpoIN_R8**	**vpoIN_R9**	**vpoIN_R10**	**vpoIN_R11**	**vpoIN_R12**	**vpoIN_R13**	**vpoIN_R14**
SAG_R#	5353954	0	0	173	17	78	0	2	3	0	0	0	0	0	0	0	0	0	0	0	0	0	0	0	0
SAG_L#	4358525	0	0	79	2	19	0	0	0	0	0	0	0	0	0	0	0	0	0	0	0	0	0	0	0
pC1a*	3807213	4	1	3	40	85	20	7	139	0	0	0	0	1	0	1	0	0	0	0	0	0	0	0	0
pC1b#	3781622	0	0	0	0	6	0	0	13	0	0	0	0	0	0	0	0	0	0	0	0	0	0	0	0
pC1c*	3794184	0	0	5	6	0	10	23	77	0	0	0	0	0	0	0	0	0	0	0	0	0	0	0	0
pC1d#	3778246	0	0	2	0	5	0	10	13	0	0	0	0	0	0	0	0	0	0	0	0	0	0	0	0
pC1e*	1269969	0	0	1	3	4	5	4	0	0	0	0	0	0	1	0	0	0	0	0	0	0	0	0	0
vpoDN*	5094165	0	0	13	6	15	18	21	2	0	0	0	0	1	0	1	0	0	0	0	0	0	0	0	0
vpoEN_R1#	5496947	0	0	0	0	5	10	2	81	0	3	0	0	0	1	0	0	0	0	0	0	0	0	0	0
vpoEN_R2#	5480915	0	0	0	0	2	5	4	62	2	0	0	0	0	0	0	0	0	0	0	0	0	0	0	0
vpoIN_R1#	5114793	0	0	1	0	4	0	42	60	0	0	0	0	0	0	2	0	0	0	0	0	0	0	0	0
vpoIN_R2#	6481209	0	0	0	0	3	0	30	54	0	0	0	0	0	1	0	0	0	0	0	0	0	0	0	0
vpoIN_R3#	5310407	0	0	0	0	3	0	19	44	0	0	1	1	0	0	0	0	0	0	0	0	0	0	0	0
vpoIN_R4#	5486635	0	0	0	0	2	0	21	42	1	0	0	0	0	0	1	0	0	0	0	0	0	0	0	0
vpoIN_R5#	1945493	0	0	0	0	3	0	14	36	0	0	0	0	0	0	0	0	0	0	0	0	0	0	0	0
vpoIN_R6#	5500623	0	0	0	1	12	0	5	29	3	4	0	0	0	0	0	0	0	0	0	0	0	0	0	0
vpoIN_R7#	7125206	0	0	0	0	4	0	8	26	0	0	0	0	0	0	0	0	0	0	1	0	1	1	0	0
vpoIN_R8#	5753207	0	0	0	0	0	0	5	24	0	0	0	0	0	0	0	0	0	0	0	0	0	0	0	0
vpoIN_R9#	5592797	0	0	0	0	8	0	5	19	0	0	0	2	0	0	0	0	0	0	0	0	0	0	0	0
vpoIN_R10#	5123561	0	0	0	0	3	0	7	9	0	1	0	0	0	1	0	0	1	0	0	0	0	0	0	0
vpoIN_R11#	6540244	0	0	0	0	0	0	0	9	1	0	0	0	0	0	0	1	0	0	0	0	0	0	0	0
vpoIN_R12#	7378248	0	0	0	0	2	0	1	5	0	0	0	0	0	0	0	0	0	0	0	0	0	0	0	0
vpoIN_R13#	5746423	0	0	0	0	0	0	2	3	0	0	0	0	0	0	0	0	0	0	0	0	0	0	0	0
vpoIN_R14#	6031289	0	0	0	1	8	0	2	3	0	0	0	0	0	0	0	0	0	0	0	0	0	0	0	0

SAG_R and SAG_L indicate right and left hemisphere SAG cells, respectively. All other neurons are right hemisphere cells. *Fully traced cells. #Partially traced cells.

nature research

Corresponding author(s): *Double-blind peer review submissions: write DBPR and your manuscript number here instead of author names.*

Last updated by author(s): *YYYY-MM-DD*

Reporting Summary

Nature Research wishes to improve the reproducibility of the work that we publish. This form provides structure for consistency and transparency in reporting. For further information on Nature Research policies, see Authors & Referees and the Editorial Policy Checklist.

Statistics

For all statistical analyses, confirm that the following items are present in the figure legend, table legend, main text, or Methods section.

n/a	Confirmed	
☐	☒	The exact sample size (*n*) for each experimental group/condition, given as a discrete number and unit of measurement
☐	☒	A statement on whether measurements were taken from distinct samples or whether the same sample was measured repeatedly
☐	☒	The statistical test(s) used AND whether they are one- or two-sided *Only common tests should be described solely by name; describe more complex techniques in the Methods section.*
☒	☐	A description of all covariates tested
☒	☐	A description of any assumptions or corrections, such as tests of normality and adjustment for multiple comparisons
☐	☒	A full description of the statistical parameters including central tendency (e.g. means) or other basic estimates (e.g. regression coefficient) AND variation (e.g. standard deviation) or associated estimates of uncertainty (e.g. confidence intervals)
☐	☒	For null hypothesis testing, the test statistic (e.g. *F*, *t*, *r*) with confidence intervals, effect sizes, degrees of freedom and *P* value noted *Give P values as exact values whenever suitable.*
☒	☐	For Bayesian analysis, information on the choice of priors and Markov chain Monte Carlo settings
☒	☐	For hierarchical and complex designs, identification of the appropriate level for tests and full reporting of outcomes
☒	☐	Estimates of effect sizes (e.g. Cohen's *d*, Pearson's *r*), indicating how they were calculated

Our web collection on statistics for biologists contains articles on many of the points above.

Software and code

Policy information about availability of computer code

Data collection	ScanImage (r2016a) from Vidrio Technologies and pCLAMP 10 from Molecular Devices were used to collect calcium imaging and electrophysiology data, respectively.
Data analysis	Open source software Fiji (v1.52p), R software (v3.6.3), CATMAID software (FAFB00, V14), pCLAMP 10 from Molecular Devices, and MATLAB (R2018b) from Mathworks were used to analyze data.

For manuscripts utilizing custom algorithms or software that are central to the research but not yet described in published literature, software must be made available to editors/reviewers. We strongly encourage code deposition in a community repository (e.g. GitHub). See the Nature Research guidelines for submitting code & software for further information.

Data

Policy information about availability of data

All manuscripts must include a data availability statement. This statement should provide the following information, where applicable:

- Accession codes, unique identifiers, or web links for publicly available datasets
- A list of figures that have associated raw data
- A description of any restrictions on data availability

Confocal images of the central nervous systems of split-GAL4 lines used in this study are available at http://splitgal4.janelia.org/cgi-bin/splitgal4.cgi. Other datasets generated during the current study are available from the corresponding author on reasonable request.

Field-specific reporting

Please select the one below that is the best fit for your research. If you are not sure, read the appropriate sections before making your selection.

☒ Life sciences ☐ Behavioural & social sciences ☐ Ecological, evolutionary & environmental sciences

For a reference copy of the document with all sections, see nature.com/documents/nr-reporting-summary-flat.pdf

Life sciences study design

All studies must disclose on these points even when the disclosure is negative.

Sample size	Samples sizes were chosen based on prior experience with similar behavioral and imaging experiments. No sample-size calculation was performed.
Data exclusions	No data were excluded.
Replication	Experiments were replicated on at least three different days. All attempts at replication were successful.
Randomization	Samples were allocated based on the corresponding genotypes.
Blinding	Investigators were not blind to group allocation during data collection, calcium imaging analysis, and electrophysiological data analysis, as these were nonsubjective. In scoring behaviors, two independent investigators were blind to the group allocation.

Reporting for specific materials, systems and methods

We require information from authors about some types of materials, experimental systems and methods used in many studies. Here, indicate whether each material, system or method listed is relevant to your study. If you are not sure if a list item applies to your research, read the appropriate section before selecting a response.

Materials & experimental systems

n/a	Involved in the study
☐	☒ Antibodies
☒	☐ Eukaryotic cell lines
☒	☐ Palaeontology
☐	☒ Animals and other organisms
☒	☐ Human research participants
☒	☐ Clinical data

Methods

n/a	Involved in the study
☒	☐ ChIP-seq
☒	☐ Flow cytometry
☒	☐ MRI-based neuroimaging

Antibodies

Antibodies used	Primary antibodies: Rabbit anti-GFP (Cat# A11122, Thermo Fisher); Rabbit anti-HA Tag (Cat# 3724S, Cell Signal Technologies); Rat anti-FLAG Tag (Cat# NBP1-06712, Novus Biologicals); rabbit anti-dsRed (Cat# 632496, Takara Bio); chicken anti-GFP (Cat# A10262, Thermo Fisher); mouse anti-Bruchpilot (nc82, DSHB). Secondary antibodies: Cy2 Goat anti-mouse (Cat# 115-225-166, Jackson Immuno Research); Cy3 Goat anti-rabbit (Cat# 111-165-144, Jackson Immuno Research); ATTO 647N Goat anti-rat (Cat# 612-156-120, Rockland); AF546-conjugated Goat anti-rabbit (Cat# A11035, Thermo Fisher); AF488-conjugated Goat anti-chicken (Cat# A32931, Thermo Fisher); AF647-conjugated Goat anti-mouse (Cat# A21235, Thermo Fisher).
Validation	All antibodies used in this study were commercially developed. Validation statement, detailed instruction, and multiple published references of each antibody used in this study are available on the manufacturers' websites listed as below. www.thermofisher.com/antibody/product/GFP-Antibody-Polyclonal/A-11122. www.thermofisher.com/antibody/product/GFP-Antibody-Polyclonal/A10262. www.cellsignal.com/products/primary-antibodies/ha-tag-c29f4-rabbit-mab/3724?Ntk=Products&Ntt=3724. www.novusbio.com/products/dykddddk-epitope-tag-antibody-l5_nbp1-06712. www.takarabio.com/products/antibodies-and-elisa/fluorescent-protein-antibodies/red-fluorescent-protein-antibodies. dshb.biology.uiowa.edu/nc82. https://www.jacksonimmuno.com/catalog/products/115-225-166. www.jacksonimmuno.com/catalog/products/111-165-144. https://rockland-inc.com/store/ATTO-Conjugated-Antibodies-612-156-120-O4L_23722.aspx. https://www.thermofisher.com/antibody/product/Goat-anti-Rabbit-IgG-H-L-Highly-Cross-Adsorbed-Secondary-Antibody-Polyclonal/A-11035. https://www.thermofisher.com/antibody/product/Goat-anti-Chicken-IgY-H-L-Cross-Adsorbed-Secondary-Antibody-Polyclonal/A32931. https://www.thermofisher.com/antibody/product/Goat-anti-Mouse-IgG-H-L-Cross-Adsorbed-Secondary-Antibody-Polyclonal/

A-21235.

Animals and other organisms

Policy information about studies involving animals; ARRIVE guidelines recommended for reporting animal research

Laboratory animals	Female and male Drosophila melanogaster aged 3-7 days were used in this study. Detailed information are provided in Extended Data.
Wild animals	This study did not involve wild animals.
Field-collected samples	This study did not involve samples collected from the field.
Ethics oversight	No ethical approval was required.

Note that full information on the approval of the study protocol must also be provided in the manuscript.